Interaction of Radiation and Fast Electrons with Clusters of Dielectrics: A Multiple Scattering Approach

F. J. García de Abajo*

Materials Sciences Division, Lawrence Berkeley National Laboratory, Berkeley, California 94720

(Received 2 November 1998)

A fast, accurate, and general technique for solving Maxwell's equations in arbitrarily disposed clusters of dielectric objects is presented, based upon multiple scattering of electromagnetic multipole fields. Examples of application to the simulation of electron energy loss, radiation emission induced by fast electrons, and light scattering are offered. Large rates of Smith-Purcell radiation are predicted in the interaction of fast electrons with strings of Al and SiO_2 spheres, suggesting its possible application in tunable soft UV light generation. Mutual electromagnetic interaction among objects in the different clusters under consideration is shown to be of primary importance. [S0031-9007(99)08761-X]

PACS numbers: 73.20.Mf, 41.20.Jb, 61.16.Bg, 61.46.+w

The electromagnetic field in composite dielectric media has recently received growing attention in connection with the characterization of nanostructures [1] and the study of scattering, reflection, and absorption of radiation [2,3]. As small microstructures are becoming feasible in the search for actual photonic materials [3], theoretical methods suited for the simulation of radiation scattering in large, arbitrarily disposed dielectric clusters are becoming necessary in the analysis of fabrication misalignment effects [4] and various other phenomena like the recently discovered photonic molecules [5] and radiation tunneling in photonic lattices [6].

Numerical methods based upon the transfer matrix approach have been recently developed by Pendry and co-workers for periodic dielectric composites [7–9]. Effective medium theories have been applied to random distributions of dielectrics [10,11]. Also, electron energy losses near arbitrarily shaped interfaces have been simulated making use of boundary charges and currents to reduce the three-dimensional Maxwell equations to two-dimensional surface integral equations [12].

A general, computationally efficient technique is presented here to solve Maxwell's equations in clusters of arbitrarily-distributed dielectrics. In a first step, the external electromagnetic field is decomposed into multipoles around each object of the cluster. Then, the self-consistent field is expressed in terms of the complex scattering matrices of the different dielectrics. Finally, multiple scattering is carried out until convergence is achieved.

Let us first consider a dielectric body placed in vacuum. The electric field can be expressed in frequency space ω in terms of longitudinal, magnetic, and electric scalar functions, ψ_α^L, ψ_α^M, and ψ_α^E, as [13]

$$\mathbf{E} = \nabla\psi_\alpha^L + \mathbf{L}_\alpha\psi_\alpha^M - \frac{\mathrm{i}}{k}\nabla\times\mathbf{L}_\alpha\psi_\alpha^E, \qquad (1)$$

where $k = \omega/c$, $\mathbf{L}_\alpha = -\mathrm{i}(\mathbf{r} - \mathbf{r}_\alpha)\times\nabla$ is the orbital angular-momentum operator, and the subscript α indicates that all coordinates are given relative to a nearby position $\mathbf{r}_\alpha$. Assuming that no external sources are located near the object, one can choose $\psi_\alpha^L = 0$, so that longitudinal modes are explicitly left out (this is a natural gauge due to the transversal nature of the electric field in this case). $\psi_\alpha = (\psi_\alpha^M, \psi_\alpha^E)$ satisfies the wave equation

$$(\nabla^2 + k^2)\psi_\alpha = 0 \qquad (2)$$

in the vacuum region.

The electromagnetic field created by some external source must have zero net energy flux around the object, where the external scalar functions can thus be expanded in terms of spherical harmonics Y_{lm} as

$$\psi_\alpha^{\mathrm{ext}}(\mathbf{r}) = \sum_{lm}\mathrm{i}^l j_l(k|\mathbf{r} - \mathbf{r}_\alpha|)Y_{lm}(\widehat{\mathbf{r} - \mathbf{r}_\alpha})\psi_{\alpha,lm}^{\mathrm{ext}}$$

and j_l is a spherical Bessel function. Besides, the induced part of the electromagnetic field $\psi_\alpha^{\mathrm{ss}}$ results from the single scattering (ss) of $\psi_\alpha^{\mathrm{ext}}$ by the object, so that it is by necessity a combination of spherical outgoing waves,

$$\psi_\alpha^{\mathrm{ss}}(\mathbf{r}) = \sum_{lm}\mathrm{i}^l h_l^{(+)}(k|\mathbf{r} - \mathbf{r}_\alpha|)Y_{lm}(\widehat{\mathbf{r} - \mathbf{r}_\alpha})\psi_{\alpha,lm}^{\mathrm{ss}}, \qquad (3)$$

for $\mathbf{r}$ outside a sphere centered at $\mathbf{r}_\alpha$ and containing the object. Here $h_l^{(+)}$ is a spherical Hankel function [14]. The relation between $\psi_\alpha^{\mathrm{ext}}$ and $\psi_\alpha^{\mathrm{ss}}$ is provided by the scattering matrix t_α, implicitly defined by $\tilde{\psi}_\alpha^{\mathrm{ss}} = t_\alpha\tilde{\psi}_\alpha^{\mathrm{ext}}$, where $\tilde{\psi}_\alpha^{\mathrm{ss(ext)}}$ is a vector of components $\psi_{\alpha,lm}^{\mathrm{ss(ext)}}$.

Now, let us focus on a cluster of dielectric objects labeled by coordinate vectors $\mathbf{r}_\alpha$. The induced part of the self-consistent scattered field is the sum of contributions coming from the different components of the cluster, that is, $\psi^{\mathrm{ind}} = \sum_\alpha \psi_\alpha^{\mathrm{ind}}$. Here, $\psi_\alpha^{\mathrm{ind}}$ takes the same form as Eq. (3), except that it is made up of $\psi_\alpha^{\mathrm{ss}}$ (single scattering of the external field at α) plus the result of the free propagation of $\psi_\beta^{\mathrm{ind}}$ from each object $\beta \neq \alpha$, followed by scattering at α (self-consistent multiple scattering). That is,

$$\lambda\tilde{\psi}_\alpha^{\mathrm{ind}} = \tilde{\psi}_\alpha^{\mathrm{ss}} + t_\alpha\sum_{\beta\neq\alpha}H_{\alpha\beta}\tilde{\psi}_\beta^{\mathrm{ind}}, \qquad (4)$$

 0031-9007/99/82(13)/2776(4)$15.00

where the operator $H_{\alpha\beta}$ describes the noted propagation and $\lambda = 1$ has been introduced for convenience. $H_{\alpha\beta}$ can be constructed in four steps:

(i) First, the bond vector $\mathbf{d}_{\alpha\beta} = \mathbf{r}_\alpha - \mathbf{r}_\beta$ is rotated onto the z axis by using a rotation matrix $R_{\alpha\beta}$ [14], which acts on the spherical harmonics of Eq. (3).

(ii) The resulting rotated scalar functions $\psi_\beta^{\rm ind}$ are then propagated a distance $|\mathbf{d}_{\alpha\beta}|$ along the positive direction of the z axis; this is accomplished by multiplying by the Green function of Eq. (2), $G^z_{\alpha\beta}$, appropriately written in the basis set of spherical harmonics attached to $\mathbf{r}_\alpha$ and $\mathbf{r}_\beta$ [15].

(iii) The scalar functions are not invariant under translations of the multipole origin, but their variation when the latter is displaced from $\mathbf{r}_\beta$ to $\mathbf{r}_\alpha$ can be described by a linear translation operator $T^z_{\alpha\beta}$ [16].

(iv) Finally, the z axis is rotated back onto the $\mathbf{d}_{\alpha\beta}$ direction, and one has

$$H_{\alpha\beta} = R^{-1}_{\alpha\beta} T^z_{\alpha\beta} G^z_{\alpha\beta} R_{\alpha\beta} \,. \tag{5}$$

The analogy with electron diffraction in solids [15,17] is complete, except for the lack of translational invariance of the scalar functions just noted [16].

For simplicity, we shall focus on clusters formed by spherically symmetric objects, for which t_α becomes diagonal and its elements can be expressed in terms of the phase shifts of magnetic and electric components as $[t_\alpha]^\nu_{lm,l'm'} = \delta_{ll'}\delta_{mm'} \sin\delta_l^{\alpha,\nu} \exp(i\delta_l^{\alpha,\nu})$, where ν stands for M and E, respectively. $\delta_l^{\alpha,\nu}$ takes particularly simple forms for homogeneous spheres [18,19] described by local dielectric functions, as those considered below. Nevertheless, the present formalism can be applied to arbitrarily shaped scatterers, for which the scattering matrices are generally dense, and can be obtained numerically [12].

The operators under consideration are approximated by finite matrices of dimension $[(l_{\rm max}+1)^2]^2$. Convergence has been obtained in most of the calculations presented below for $l_{\rm max} = 8$.

The direct inversion of Eq. (4) is computationally prohibitive for large clusters. Here, it has been solved by using the recursion method, where λ plays the same role as the energy in former electronic band-structure calculations [20]. The recursion method, unlike the Taylor expansion of $\tilde{\psi}_\alpha^{\rm ind}$'s in powers of t_α's, is fully convergent in the present context.

The matrices on the right hand side of Eq. (5) are all sparse. Actually, this factorization reduces both the storage demand and the computation time by a factor of $\approx l_{\rm max}/2$. Notice that multiplication by scattering matrices does not affect significantly the total computational costs for relatively large clusters (e.g., above ten objects), since it takes place just outside the summation over cluster objects in Eq. (4). Furthermore, for any arbitrary cluster, one can choose the points $\mathbf{r}_\alpha$ in such a way that they form a highly symmetrical mesh, where many bond distances and angles are repeated (this might require that the points $\mathbf{r}_\alpha$ are not in the geometrical centers of the objects that they label), so that the total number of inequivalent matrices $R_{\alpha\beta}$, $G^z_{\alpha\beta}$, and $T^z_{\alpha\beta}$ is substantially smaller than the number of different $H_{\alpha\beta}$'s; thus, a large reduction in computational effort is achieved by calculating each of those matrices only the first time that it is encountered along the full calculation. Further decomposition of rotation matrices into azimuthal and polar rotations helps in this respect.

A fully automated implementation of these ideas has been performed [16], resulting in a new code that provides the solution of Eq. (4) investing a computation time $\approx AN^2(l_{\rm max}+1)^3$, where N is the number of dielectric objects in the cluster and A is a constant ($A \sim 10^{-4}$ sec on a Pentium at 333 MHz).

Next, the present formalism is applied to the simulation of electron energy loss, radiation emission induced by fast electrons, and radiation scattering in different clusters of SiO_2 and Al spheres. The dielectric function of SiO_2 is taken from optical data [21] and a Drude expression is used for Al with a plasma energy of 15 eV and a damping of 1.06 eV.

The coefficients $\psi^{\rm ext}_{\alpha,lm}$ take analytical forms when the external field is produced by an electron moving with constant velocity [19]. The energy loss probability has been derived from the retarding force produced by the induced electric field acting back on the electron [12], which is in turn calculated analytically from Eq. (1) and the coefficients $\psi^{\rm ind}_{\alpha,lm}$ obtained from Eq. (4). Probabilities for photon emission induced by fast electrons have been obtained by integrating the Poynting vector normal to a large sphere centered at the cluster.

Figure 1 illustrates the energy loss and induced photon emission probabilities for fast electrons moving with constant velocity parallel to an infinite periodic string of aligned spheres, as shown in Fig. 1(a). Smith-Purcell radiation [22,23] is emitted under these conditions along angles θ with respect to the string direction such that the phase of the far fields originating in contiguous spheres differs in a multiple of 2π, that is, $\omega d/c(\cos\theta - c/v) = 2\pi n$, where d is the string period, v is the electron velocity, ω is the radiation frequency, and n is a negative integer. Figures 1(b)–1(c) show the emission probability per sphere and energy range for $n = -1$ and $n = -2$ in the cases of SiO_2 and Al spheres (solid curves), respectively. For each n, there is an emission threshold energy when $\theta = \pi$. The energy loss probability per sphere (dashed curves) follows the emission probability in the case of SiO_2 [Fig. 1(b)] within the region below 8.5 eV, where the imaginary part of the dielectric function is very small and most of the energy loss is converted into Smith-Purcell radiation, leading to an absolute threshold for energy losses at $\hbar\omega_0 = \hbar(2\pi c/d)/(c/v+1)$ ($\approx$4.24 eV under the conditions of the figure). For Al spheres [Fig. 1(c)], part of the energy loss goes always into absorption. In particular,

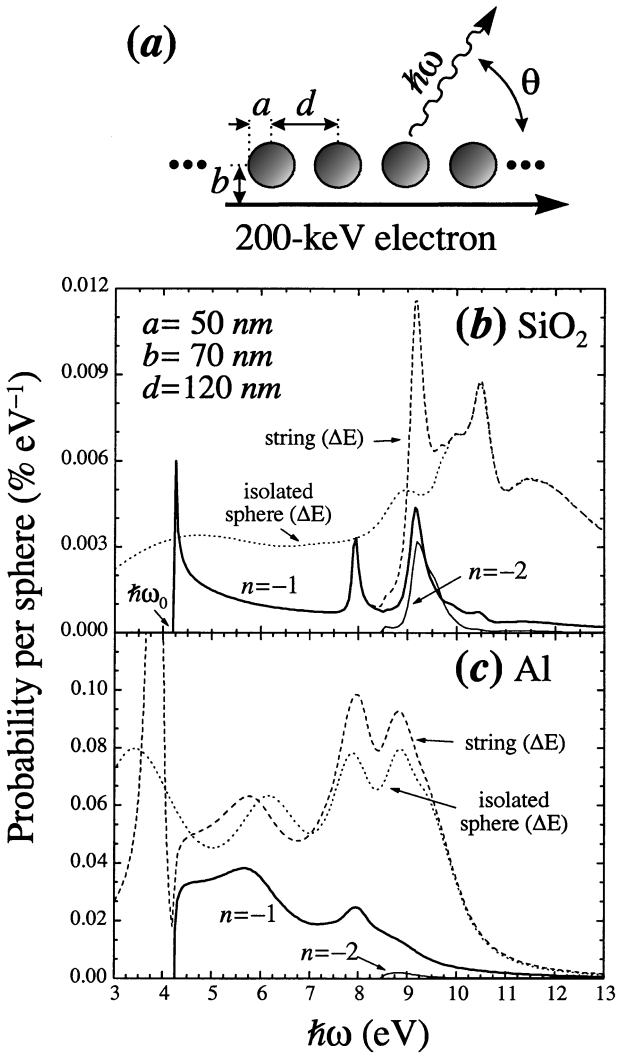

FIG. 1. Energy loss probability and Smith-Purcell radiation emission for an electron moving parallel to an infinite periodic string of aligned spheres, as shown in (a). Two different materials have been considered: (b) SiO_2 and (c) Al. The photon emission probability per sphere and energy range $\hbar\omega$ is represented by solid curves for the first and second harmonics ($n = -1, -2$). Energy loss spectra are represented by dashed curves. Energy loss spectra for an isolated sphere are shown by dotted curves for the same velocity and impact parameter.

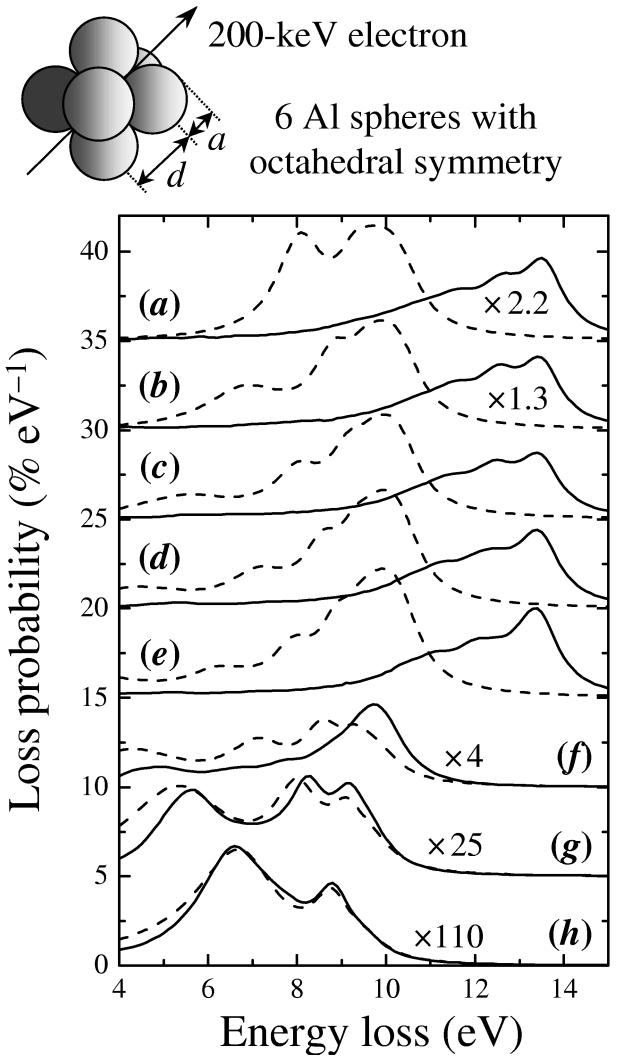

FIG. 2. Electron energy loss probability per energy range for an electron passing by the center of an octahedral cluster of Al spheres. Single scattering results (dashed curves, noninteracting spheres) and full multiple scattering results (solid curves) are shown for clusters of touching spheres with bond distances $d =$ 20, 40, 60, 80, and 100 nm in (a)–(e), respectively. Curves (f)–(h) correspond to clusters with constant bond distance $d =$ 100 nm and sphere radius $a = 40$, 30, and 20 nm, respectively. The electron trajectory is chosen to intersect the centers of two opposite edges of the imaginary octahedrum that defines the geometry. Some of the curves have been multiplied by a factor, as shown in the figure, and consecutive curves have been shifted 5% eV^{-1} upwards to improve readability.

this happens in the energy loss peak at 3.8 eV (below the emission threshold), which can be ascribed to the excitation of an intrinsic mode of the string. However, the radiation emission probability is higher in the Al case for $n = -1$ as compared to silica. The energy loss probability for an isolated sphere (dotted curves) follows the loss probability in the string at high emission energies, where coupling between spheres plays a minor role.

The interaction among the objects of a cluster can produce dramatic effects in the energy loss spectra of fast electrons passing nearby, as shown in Fig. 2 for octahedral clusters of Al spheres. The spectra calculated without taking into account this interaction (broken curves) are very different from the full multiple-scattering results (solid curves) in the case of touching spheres [see Figs. 2(a)–2(e) for clusters of increasing size]. Notice in particular the extinction of losses below 9 eV. As the distance between sphere surfaces is increased, the interaction among spheres becomes less important as shown in Figs. 2(e)–2(h) for clusters with the same bond distance and decreasing sphere radii.

The effect of multiple scattering of external radiation in a cluster of dielectric objects is illustrated in Fig. 3, where the radiation scattering cross section is represented

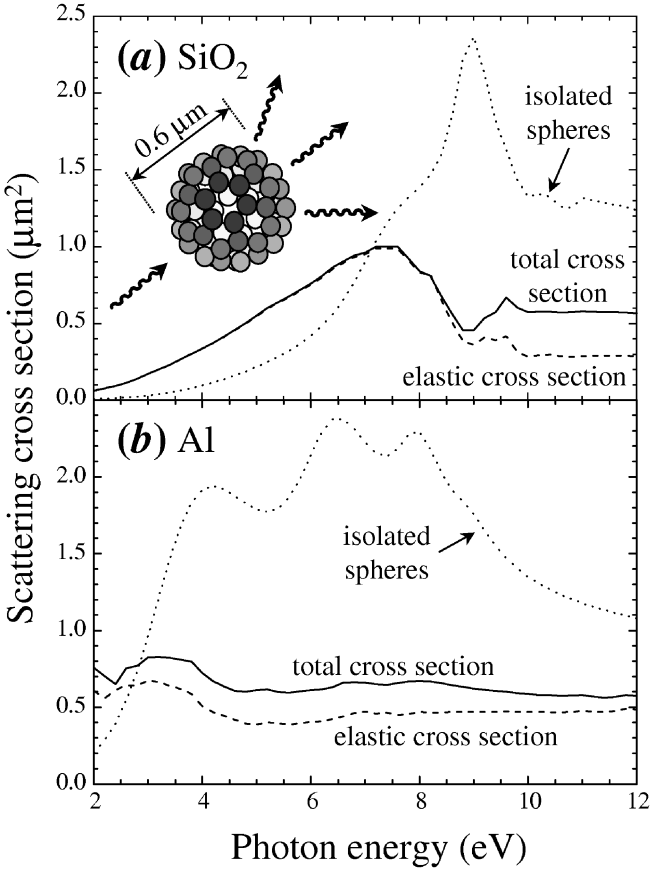

FIG. 3. (a) Radiation scattering cross section for a cluster formed by 60 SiO_2 spheres with the same structure as carbons in a C_{60} molecule. The radius of the spheres is 49.5 nm. The nearest neighbors bond distance is 100 nm. The elastic cross section (dashed curve) is compared with the total cross section (solid curve) and 60 times the total cross section of an isolated sphere (dotted curve). (b) The same as (a) for Al spheres.

for a cluster of 60 spheres with the same structure as carbons in a C_{60} molecule. For SiO_2 spheres [Fig. 3(a)], the total scattering cross section (solid curve, including photon absorption processes), calculated by using the optical theorem for light [13], follows quite closely the elastic scattering cross section (dashed curve) in the region below $\approx$8.5 eV, where absorption is negligible. Elastic scattering cross sections have been obtained by integrating the scattered radiation over angles of scattering. For Al spheres [Fig. 3(b)], both cross sections are relatively featureless. In silica, the prominent feature obtained for single scattering at around 9 eV (dotted curve, representing 60 times the total cross section of an isolated sphere) is converted into a dip when multiple scattering is switched on.

In summary, a general and computationally efficient technique has been presented for solving Maxwell's equations in a cluster of arbitrarily disposed dielectric objects. Examples of application to the simulation of electron energy loss and radiation scattering have been considered. For an electron moving parallel to a periodic infinite chain of dielectric spheres, large Smith-Purcell radiation emission probabilities have been predicted, raising the possibility of using this effect to produce tunable UV light. The theory presented here can help to extract geometrical and chemical information on complex dielectric clusters by analyzing radiation scattering and electron energy loss spectra.

The author wants to thank A. Howie, P. M. Echenique, and R. Fuchs for helpful and enjoyable discussions, and M. A. Van Hove and C. S. Fadley for their kind hospitality. Help and support from the University of the Basque Country, the Spanish Ministerio de Educación y Cultura under Fulbright Grant No. FU-98-22726216, and the U.S. DOE under Contract No. DE-AC03-76SF00098 are gratefully acknowledged.

*Permanent address: Departamento de CCIA (Facultad de Informática), Donostia International Physics Center (DIPC), and Centro Mixto CSIC-UPV/EHU, San Sebastián, Spain.

[1] A. Howie and C. Walsh, Microsc. Microanal. Microstruct. **2**, 171 (1991).
[2] P. M. Hui and N. F. Johnson, Solid State Phys. **49**, 151 (1995).
[3] J. D. Joannopoulos, P. R. Villeneuve, and S. Fan, Nature (London) **386**, 143 (1997).
[4] H. Li, B. Cheng, and D. Zhang, Phys. Rev. B **56**, 10 734 (1997).
[5] M. Bayer *et al.*, Phys. Rev. Lett. **81**, 2582 (1998).
[6] S. Fan, P. R. Villeneuve, J. D. Joannopoulos, and H. A. Haus, Phys. Rev. Lett. **80**, 960 (1998).
[7] J. B. Pendry and A. MacKinnon, Phys. Rev. Lett. **69**, 2772 (1992).
[8] J. B. Pendry and L. Martín-Moreno, Phys. Rev. B **50**, 5062 (1994).
[9] F. J. García-Vidal, J. M. Pitarke, and J. B. Pendry, Phys. Rev. Lett. **78**, 4289 (1997).
[10] L. Fu and L. Resca, Phys. Rev. B **47**, 16 194 (1993).
[11] R. G. Barrera and R. Fuchs, Phys. Rev. B **52**, 3256 (1995).
[12] F. J. García de Abajo and A. Howie, Phys. Rev. Lett. **80**, 5180 (1998).
[13] F. E. Low, *Classical Field Theory: Electromagnetism and Gravitation* (John Wiley & Sons, New York, 1997).
[14] A. Messiah, *Quantum Mechanics* (North-Holland, New York, 1966).
[15] J. B. Pendry, *Low Energy Electron Diffraction* (Academic Press, London, 1974).
[16] F. J. García de Abajo (to be published).
[17] J. J. Rehr and R. C. Albers, Phys. Rev. B **41**, 8139 (1990).
[18] K. Ohtaka and M. Inoue, Phys. Rev. B **25**, 677 (1982).
[19] F. J. García de Abajo, Phys. Rev. B **59**, 3095 (1999).
[20] R. Haydock, Solid State Phys. **35**, 215 (1980).
[21] E. D. Palik, *Handbook of Optical Constants of Solids* (Academic Press, New York, 1985).
[22] S. J. Smith and E. M. Purcell, Phys. Rev. **92**, 1069 (1953).
[23] J. Urata *et al.*, Phys. Rev. Lett. **80**, 516 (1998).